Inverse Design of Integrated Photonic Devices by Reshaping Silicon Waveguide

1st,# Yuanhang Ren
School of Information and Communication Engineering, Beijing University of Posts and Telecommunications
Beijing 100876, China
 # These authors contribute equally
renyh@bupt.edu.cn

2nd,# Xinyu Luo
State Key Laboratory of Information Photonics and Optical Communications, Beijing University of Posts and Telecommunications
Beijing 100876, China
 # These authors contribute equally
lxy_517@bupt.edu.cn

3rd Han Ye
State Key Laboratory of Information Photonics and Optical Communications, Beijing University of Posts and Telecommunications
Beijing 100876, China
Han_ye@bupt.edu.cn

***Abstract*—Based on shape optimization of silicon waveguide, we propose three mode converters and five power splitters. The function regions occupy only 4×1 μ m2 and 6×1 μ m2 for mode converter and power splitter, respectively.**

Keywords—Integrated optics devices, All-optical devices, Waveguides

I. Introduction

With the rapid development of the digital information era, people have an unprecedented demand for the optical fiber communication system's transmission capacity and rate. Therefore, the photonic devices in the optical fiber communication network must develop towards the direction of large bandwidth, miniaturization, low loss, high efficiency, and integration. However, traditional optical devices' physical support and structural design are limited. Integrating them flexibly and highly is challenging, which hinders the application of these devices in photonic integrated circuits [1-3]. A new intelligent algorithm has been discovered to solve this problem and used to integrate and optimize optical waveguides. The integrated optical waveguide designed with a unique shape optimization algorithm guarantees quite a lot of information transmission capability of the waveguide. It breaks through the limitations of conventional optical devices to achieve the smaller size and more powerful photonic integrated circuits that traditional design algorithms cannot reach [4-7]. In this paper, we propose a new shape optimization algorithm and design two new photonic devices. One can achieve the function of mode conversion, including TE0-to-TE0, TE0-to-TE1, and TE0-to-TE2, and the other can achieve a specific power distribution ratio, including 90/10, 80/20, 70/30, 60/40, and 50/50. The proposed photonic device shows exceptionally high conversion efficiency, compact size, high mode purity, low loss, and other characteristics.

II. Design and Method

Both of these photonic devices are composed of ordinary silicon waveguides. As shown in Fig. 1 (a), the power splitter is a 1×2 optical coupler, and the input port is consistent with the mode converter, which is single 3μm×0.4μm rectangular waveguide, the output end is composed of two 3μm×0.4μm rectangular waveguides, used to output two lights with a specified power distribution ratio, one of which is initially 6μm×1μm deformed waveguide is used to realize the two separate beams are allocated with a specific power ratio. As shown in Fig. 1(b), the mode converter is a rectangular waveguide, the input port is a single 3μm×0.4μm rectangular waveguide, and the output port is a single 3μm×1μm rectangular waveguide. A deformed waveguide connects the input port and output port, initially a rectangle of 4μm×1μm, and is deformed by shape optimization under different output modes to achieve mode conversion. The black pixels in the two figures represent silicon (refractive index n=$\sqrt{12}$).

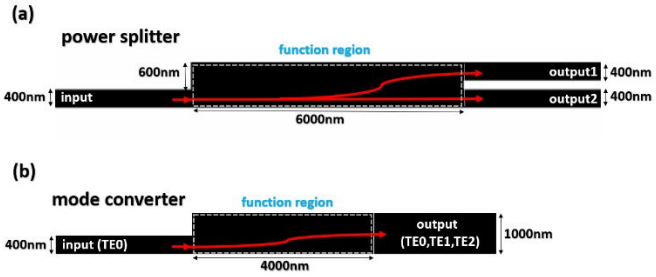

Fig. 1. (a) The power splitter design model diagram. (b) The mode converter design model diagram.

In the process of inverter design, the two-dimensional (2D) finite element method (FEM) is adopted to simulate the optical field and transmission characteristics of the reconfigurable mode converter and power splitter. The setting corresponds to planar waveguides of infinite thickness. An approach based on the method of moving asymptotes (MMA) gradient is applied to minimize the objective function, which accounts for the targeted device functionality, where λ=1550nm. The method employs a numerical analysis using Bernstein polynomials to control the variation of the polynomial boundaries in the shape optimization domain. Only under 100 optimization iterations are allowed to obtain the optimal shape of the target mode transition and power splitter.

III. Results

Combining the finite element method and the method of moving asymptotes, we can effectively find power splitters with different splitting ratios. As shown in Fig. 2(a), the 90/10 power splitting ratio is adopted as an example at the wavelength of 1550 nm. We can observe that the objective function decreases rapidly at the initial stage, and the decrease gradually slows down after 5 MMA iterations. It takes 45 iterations to reach convergence and the optimum waveguide shape. Compared with other non-gradient

algorithms, the efficiency advantage of the adopted scheme is apparent. Meanwhile, we have plotted the power flux distribution of each optimization step in Fig. 2(b), from which we can observe the whole optimization process.

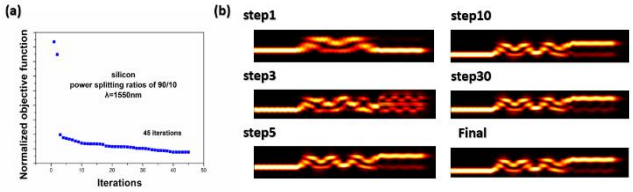

Fig. 2. Power splitter with splitting ratios of 90/10 (a)Convergence schematic. (b) The power flux distribution of several steps in the optimization progress.

Fig. 3 shows a plot of the results for the five power splitters. The power flux at the central wavelength 1550nm (X direction) and the optimized final waveguide shape are being simulated. As shown in Fig. 3(a). we can observe that the energy flux of the power splitter is relatively unstable in the function region. However, the maximum power flux remains stable in the subsequent corresponding output silicon waveguide. From the power fluxes in Fig. 3(b), The difference between the outcomes increases as the partition rate ratio gap becomes broader. But the energy loss is generally low, and the output consequent ratios are as expected.

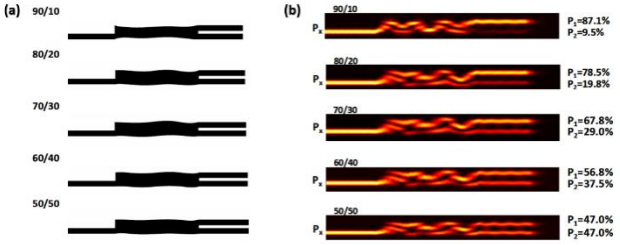

Fig. 3. Splitting ratios of 90/10, 80/20, 70/30, 60/40, 50/50 for power splitters (a) Waveguide shape after optimization. (b)The simulated power flux at the central wavelength of 1550 nm.

Fig.4 is the iterative process of the TE0-to-TE2 shape optimization algorithm. Fig.4 (a) shows the relationship between the normalized objective function value and the number of iterations during shape optimization, and Fig.4 (b) shows the change of power flux (X direction) distribution with the optimization process during the iteration process. The optimization algorithm has carried out a total of 29 iterations. At the beginning of the iteration, the value of the objective function dropped rapidly, and the power flux distribution was relatively chaotic. The value of the objective function has fallen to 90% of the initial value by the fifth iteration, and the power flux has taken shape. After that, the value of the function gradually decreased and stabilized. After 20 iterations, the value of the objective function does not change. After 29 iterations, the optimization tolerance is less than the set value, the value of the objective function reaches the set minimum value, the power flux distribution is uniform, and the shape optimization is over.

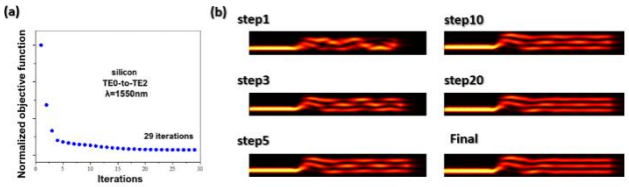

Fig. 4. Iterative process of TE0-to-TE2 shape optimization algorithm (a) convergence schematic. (b) The power flux distribution of several steps in the optimization progress.

Fig.5 is the resulting diagram of the mode converter. Fig.5 (a) shows the waveguide state in which we can achieve the conversion effect after shape optimization in the three modes of the mode converter. Fig.5 (b) shows the magnetic field intensity in the Z direction and the power flux in the X direction when the center wavelength of the left incident wave is 1550nm in the three modes of the mode converter. Taking TE0-to-TE1 as an example, the TE0 mode magnetic field presents a row of ellipses arranged perpendicular to the horizontal direction of the waveguide width. We can see from the magnetic field distribution that the shape of the magnetic field is optimized to produce deformation in the function region. The ellipse is divided into two lines in the function region and finally into two lines on the right side of the elliptical magnetic field. This indicates that the mode conversion has been completed in the function region. The power flux diagram can also reflect this feature. The number of bright flux stripes in the waveguide in the left and correct areas of the function region reflects the magnetic field mode in the waveguide. After the TE0 mode reaches the function region in the forward direction, the single-peak power flux is gradually divided into two peaks. In the subsequent silicon waveguide, the double-peak power flux keeps stable propagation, realizing the conversion of mode TE0 to TE1. The principle of mode TE0 conversion TE0 and TE2 is the same. After different shape optimization, the function region converts the wave of TE0 mode into different modes.

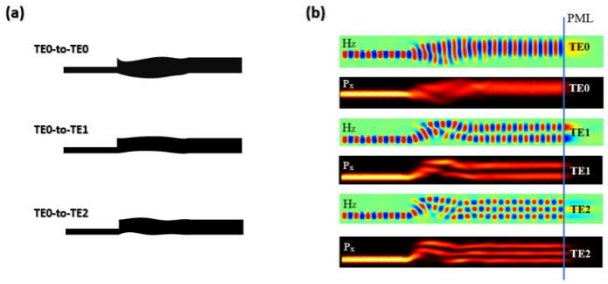

Fig. 5. Mode converter of TE0-to-TE0, TE0-to-TE1 and TE0-to-TE2 (a) Waveguide shape after optimization. (b)The simulated electric field and power flux at the central wavelength of 1550 nm.

IV. Conclusions

In summary, an inverse design method of photonic devices based on waveguide shape optimization is proposed. Multiple mode converters and power splitters with arbitrary power distribution are presented by topological design, which achieves high transmission efficiency and high purity mode conversion with a relatively minor function region footprint. Moreover, the design scheme requires fewer iterations and shorter computation time. The proposed

design approach will play an essential role in all-optical on-chip interconnects.

REFERENCES

[1] Y. Qiu, J. Tao, Z. Liu, and X. Li, ‘‘Broadband mode converter and multiplexer based on dielectric-loaded plasmonic waveguides,’’ Curr Appl Phys 20(2), 242−247 (2020).

[2] Z. Liu, X. Liu, Z. Xiao, C. Lu, H. Q. Wang, Y. Wu, X. Hu, Y. C. Liu, H. Zhang, and X. Zhang, ‘‘Integrated nanophotonic wavelength router based on an intelligent algorithm,’’ Optica 6(10), 1367−1373 (2019).

[3] H. Guan, Y. Ma, R. Shi, A. Novack, J. Tao, Q. Fang, A. E.-J. Lim, G.-Q. Lo, T. Baehr-Jones, and M. Hochberg, ‘‘Ultracompact silicon-on-insulator polarization rotator for polarization-diversified circuits,’’ Opt. Lett. 39(16), 4703−4706 (2014).

[4] H. Xu, X. Li, X. Xiao, P. Zhou, Z. Li, J. Yu, and Y. Yu, ‘‘High-speed silicon modulator with band equalization,’’ Opt. Lett. 39(16), 4839−4842 (2014).

[5] J. Wang, P. Chen, S. Chen, Y. Shi, and D. Dai, ‘‘Improved 8-channel silicon mode demultiplexer with grating polarizers,’’ Opt. Express 22(11), 12799−12807 (2014).

[6] W. Shin, and S. Fan, ‘‘Accelerated solution of the frequency-domain Maxwell’s equations by engineering the eigenvalue distribution.’’ Opt. Express 21, 22578 − 22595 (2013).

[7] Y. Wang, J. Li, M. Wang, S. Zhang, Y. Liu, and H. Ye, ‘‘Waveguide-integrated digital metamaterials for wavelength, mode and polarization demultiplexing,’’ Opt. Mater. 122, 111770 (2021).